AN EXPERIMENTAL STUDY ON MICRO-SCALE FLOW BOILING HEAT TRANSFER

Cristiano B. Tibiriçá and Gherhardt Ribatski*

* Corresponding author: Tel.: +55 (16) 3373 9415; Email: ribatski@sc.usp.br
Escola de Engenharia de São Carlos, University of São Paulo, Av. Trabalhador São Carlense, 400, São Carlos, SP, Brazil.

Abstract New experimental flow boiling heat transfer results in micro-scale tubes are presented in this paper. The experimental data were obtained in a horizontal 2.32 mm I.D. stainless steel tube with heating length of 464 mm, R245fa as working fluid, mass velocities ranging from 50 to 500 kg/m^{2}s, heat flux from 5 to 55 kW/m^2, exit saturation temperatures of 22, 31 and 41 ^{o}C, and vapor qualities from 0.05 to 0.99. Flow pattern characterization was also performed from images obtained by high speed filming. Heat transfer coefficient results from 2 to 6 kW/m^{2}K were measured. It was found that the heat transfer coefficient is a strong function of the heat flux, mass velocity and vapor quality. The experimental data were compared against the following micro-scale flow boiling predictive methods from the literature: Bertsch et al. (2008), Saitoh et al. (2007), Kandlikar and Balasubramanian (2004), Zhang et al. (2004), Thome et al. (2004) and Liu and Winterton (1991). Although not satisfactory, Thome et al. (2004) worked the best when predicting the present database.

Keywords: Micro-channel, Mini-channel, Flow Boiling, Heat Transfer

1. Introduction

Flow boiling heat transfer inside channels having hydraulic diameters less than 3mm, identified here as micro-scale channels, has been studied since the late 1950s (Lowdermilk et al. 1958), but only in recent years it has turned into a major research topic in the thermal fluid science field. Most of this interest is driven by the industrial demand for compact devices capable of dissipating extremely high heat fluxes such as those expected for the next microprocessor generation.

In this paper, new micro-scale flow boiling heat transfer results are presented. Extreme care was exercised in order to perform accurate heat transfer coefficient measurements. Flow boiling experiments were performed for R245fa in a horizontal stainless tube with and internal diameter of 2.32 mm and 464mm long. The main heat transfer trends were identified and discussed taking into account two-phase flow visualizations. The experimental results were compared against the leading micro-scale flow boiling predictive methods.

2. Experiments

2.1 Test apparatus and experimental procedure

The experimental setup is comprised of refrigerant and ethylene-glycol circuits. In the refrigerant circuit (see Fig. 1), starting from the subcooler 1, the test fluid flows through the filter to the micropump. Downstream the micropump, a bypass piping line containing a needle-valve is installed so that together with a frequency controller on the micropump the desired liquid flow rate can be set. There is then a Coriolis mass flow meter and the subcooler 2 to assure that the fluid entering the pre-heater is subcooled. Just upstream the pre-heater inlet, the enthalpy of the liquid is estimated from its temperature T_l by a 0.25mm thermocouple within the pipe and its pressure p_l by an absolute pressure transducer.

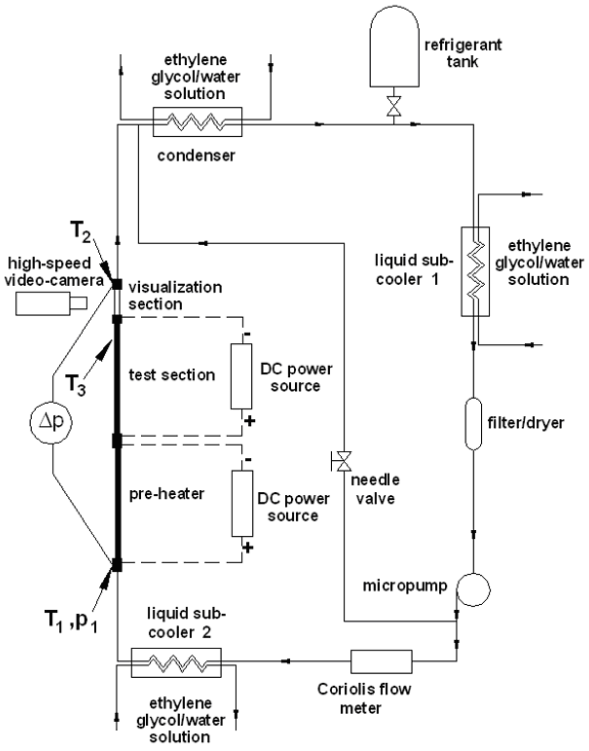

Figure 1. Schematic diagram of the refrigerant circuit.

At the pre-heater, the fluid is heated up to the desired condition at the test section inlet. The pre-heater and the test section are horizontal stainless steel tubes with an internal diameter of 2.32mm and 464mm long. The internal diameter was measured using a caliper at the open end of the tube. Both are heated by applying direct DC current to their surface and are thermally insulated. Their internal surface roughness was measured by a surface profiler using an open tube and a value of 0.33 μm was found for the mean absolute roughness, R_a. The power is supplied to the pre-heater and the test section by two independent DC power sources. The visualization section is a horizontal fused silica tube with an inner diameter of 2.1mm, a length of 85 mm, and is located just downstream to the test section. The pre-heater, the test section and the flow visualization section are connected through junctions made of electrical insulation material. Once the liquid leaves the visualization section its temperature T_2 is determined from a 0.25 mm thermocouple within the pipe. The corresponding absolute pressure is estimated from a differential pressure transducer that gives the total pressure drop between the pre-heater inlet and the flow visualization section outlet, Δp. Then, the working fluid is directed to the tube-in-tube type heat exchanger where it is condensed and subcooled. The refrigerant tank containing a serpentine coil operates as a reservoir of the working fluid and is used to control the saturation pressure in the refrigerant circuit. The saturation pressure is set by adjusting the temperature of the anti freezing ethylene glycol aqueous solution that flows through the serpentine coil within the tank.

Wall temperatures are measured through 0.25 mm type K thermocouples fixed along the test section. Rubber o-rings having an internal diameter smaller than the test section are used to fix the thermocouples on the surface by pressuring them against the tube wall. At each measuring cross-section, the surface temperature is read at three locations as indicated in Fig. 2.

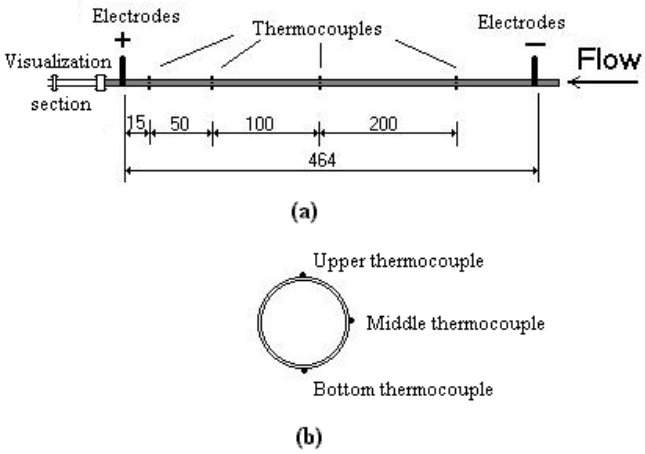

Figure 2. Details of the test section and thermocouples positioning along its surface.

The experiments were conducted first by setting the temperature in the refrigerant tank. Once established the saturation pressure in the refrigerant circuit by controlling the temperature in the refrigerant tank, the mass velocity was set through a frequency controller acting on the micropump. Then, the desired experimental heat flux is imposed to the test section and by varying the power supplied to the pre-heater, experimental results are obtained for distinct vapor qualities, keeping

the remaining parameters fixed. The datum points were logged only under steady-state conditions characterized by temperature measurement variations within the error range for at least 2 minutes.

2.2 Data reduction procedure

Heat transfer coefficient. Local heat transfer coefficients are calculated according to the Newton's cooling law as follow:

$$h_{local} = \frac{q}{T_w - T_{sat}(z)} \quad (1)$$

where T_w is the surface temperature of the inner tube wall estimated according to the Fourier's law based on the outer wall temperature measurements, and assuming both one-dimensional conduction and adiabatic external surface. T_{sat} is the local saturation temperature of the refrigerant. To estimate this temperature, firstly, based on the heat flux and on the measured temperature and pressure at the pre-heater inlet, the subcooled region length, the single-phase pressure drop over its length, and the saturation temperature at the beginning of the saturated region were calculated by solving simultaneously an equation of state relating p_{sat} and T_{sat} plus energy balance and single-phase pressure drop equations. The overall pressure drop over the saturated region is then determined by subtracting the single-phase pressure drop from the measured total pressure drop, Δp. Subsequent, a constant pressure drop gradient given by the ratio of the overall pressure drop over the saturated region and its length is assumed. After that, T_{sat} is calculated from the estimated local saturation pressure. The heat flux, q, is calculated as the ratio between the electrical power supplied to the test section and its internal area based on the heated length.

The perimeter-average heat transfer coefficient at each cross-section is calculated as follow:

$$\overline{h(z)} = \frac{h_{top}(z) + 2 \cdot h_{middle}(z) + h_{bottom}(z)}{4} \quad (2)$$

Vapor quality. The local vapor quality, $x(z)$ is obtained from energy balances over the pre-heater and the test section

2.3 Experimental validation

Compressible volume instabilities also termed in the literature by "explosive boiling" (as in Hetsroni et al. 2005) are a common phenomenon in micro-scale flow boiling. These instabilities can promote severe pressure and temperature oscillations in the flow and seems related to some of discrepancies observed when comparing experimental results from different authors (see Consolini et al. 2007). During the present experimental work, such instabilities were observed and their effects on the fluctuations of the fluid temperature and pressure were kept within the uncertainty range of instruments measurements.

Single-phase flow experiments were performed in order to assure the accuracy of the estimated vapor quality and evaluate the effective rate of heat transferred to the single phase refrigerant, $(\Delta E/E)$, defined as follow:

$$\left(\Delta E / E\right) = \frac{\left[\left[\left(\pi D^2\right)/4\right] G\left(i_{out} - i_{in}\right)\right] - \left(P_1 + P_2\right)}{P_1 + P_2} \quad (3)$$

As one can see in Fig. 3, the single-phase heat losses decrease with increasing the mass velocity with an effective rate of heat transferred to the refrigerant lower than 10% for $G \geq 100$ kg/m^{2}s and than 5% for $G \geq 400$ kg/m^{2}s. Reasonable heat losses are observed for $G = 50$ kg/m^{2}s.

Temperature measurements were calibrated and the temperature uncertainty evaluated according to the procedure suggested by Abernethy and Thompson (1973). Uncertainties for the calculated parameter were estimated using the method of sequential perturbation according to Moffat (1988). The experimental uncertainties are listed in Table 1.

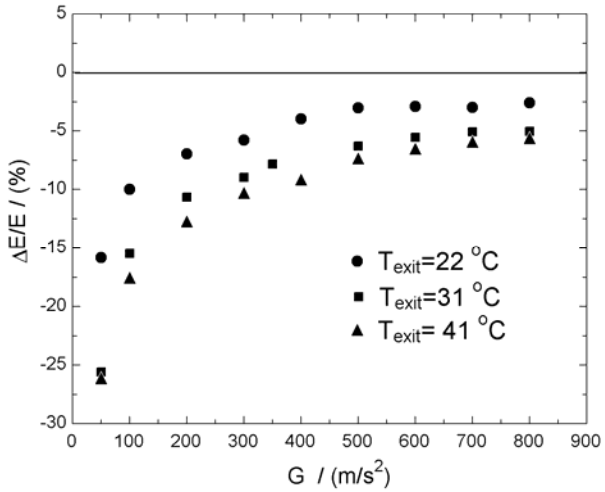

Figure 3. Evaluation of the effective rate of heat transferred to the single-phase flow refrigerant (T_{inlet}= 15 °C).

Table 1. Uncertainty of measured and calculated parameters.

Parameter	Uncertainty	Parameter	Uncertainty
D	20 μm	p	2 kPa
L	1 mm	Δp	150 Pa
G	0.8%	P_1,P_2	0.88%
h	<30%	T	0.15 °C
x	<5%		

The experimental heat transfer coefficient mean absolute uncertainty was 17.5% calculated based on the total of 700 experimental data points. In the case of data for mass velocity higher than 200 kg/m^{2}s (480 data points) the mean absolute uncertainty was of 7.1%.

In order to evaluate the accuracy of the measurements and validate the flow boiling results, single-phase heat transfer experiments were also performed and compared against the results provided by the Gnielinski (1976) correlation. Figure 4 shows that the measured single-phase heat transfer coefficient agree reasonably well with those predicted by the correlation.

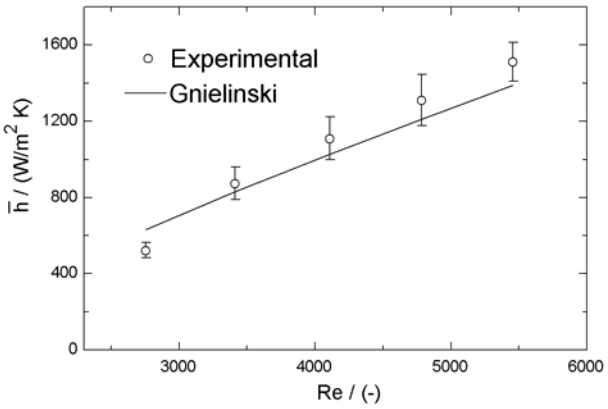

Figure 4. Comparison between the experimental and predicted single-phase heat transfer coefficients (T_{exit}= 39°C).

3. Experimental Results

3.1 Heat transfer coefficient along the tube perimeter

Figure 5 displays heat transfer coefficient measurements on the top, middle and bottom of the test tube for the thermocouples located 15 mm far from the end of the heated region of the test section. Average heat transfer coefficients given by Eq. (2) are also shown. A picture of the two-phase flow for G=200 kg/m^{2}s, q= 5kW/m^2 and x= 15% is also presented. This picture was obtained in the visualization section by high speed filming at a position located just 50 mm downstream of the heat transfer measurements. Based on the high speed filming, all heat transfer results displayed in Fig. 5 were classified as annular flows. According to this figure, stratification effects are present and a thicker liquid film is observed in the tube bottom region. This can explain the higher heat transfer coefficients on the top tube regions. According to Figs. 5a and 5b the heat transfer coefficient differences along the tube perimeter decrease with increasing mass velocity and vapor quality.

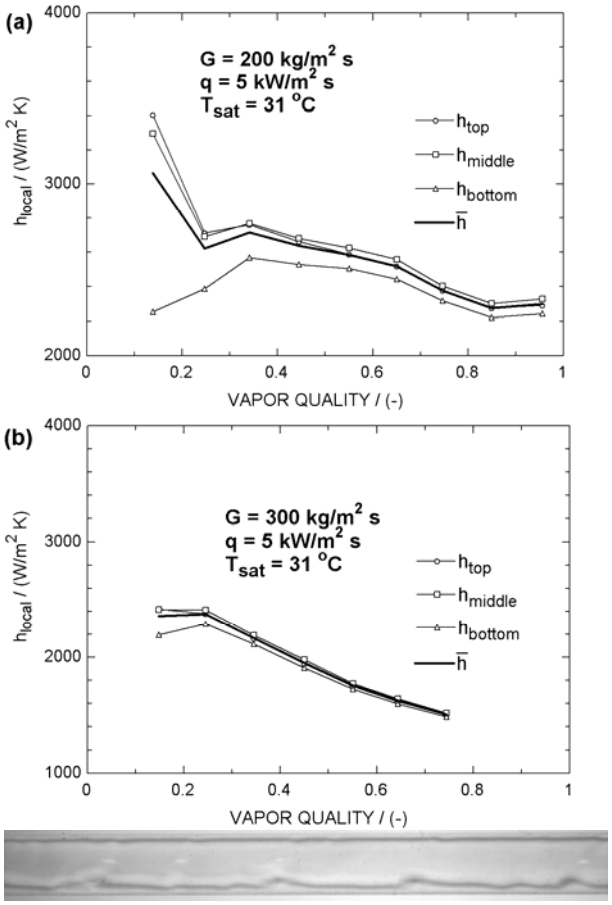

Figure 5. Heat transfer coefficient distribution along the tube perimeter measured by the thermocouples nearest from the visualization section and the two-phase flow structure for G=200 kg/m^{2}s, q=5kW/m^2, x= 15% T_{sat}=31^{o}C.

3.2 Parametric study

In this item, a parametric investigation of the effect of the experimental variables on the heat transfer coefficient is presented. In this analysis, only perimeter-average heat transfer coefficients defined according to Eq. (2) are considered.

Mass velocity. Figure 6 illustrates the effect of the mass velocity on the heat transfer coefficient at different heat flux levels for T_{sat}=31^{o}C. In general, according to this figure, the heat transfer coefficient decreases with increasing the mass velocity. Such a behavior is different from that observed by Tibiriçá and Ribatski (2009) working with R134a in the same test facility. As the vapor quality increases, this effect seems to become more pronounced. Distinct heat transfer behaviors with increasing vapor quality are observed. For the lowest heat flux the heat transfer coefficient decreases with increasing vapor quality over the entire range of vapor quality. For the highest and intermediate heat fluxes, the heat transfer coefficient has a tendency to increase with increasing vapor quality.

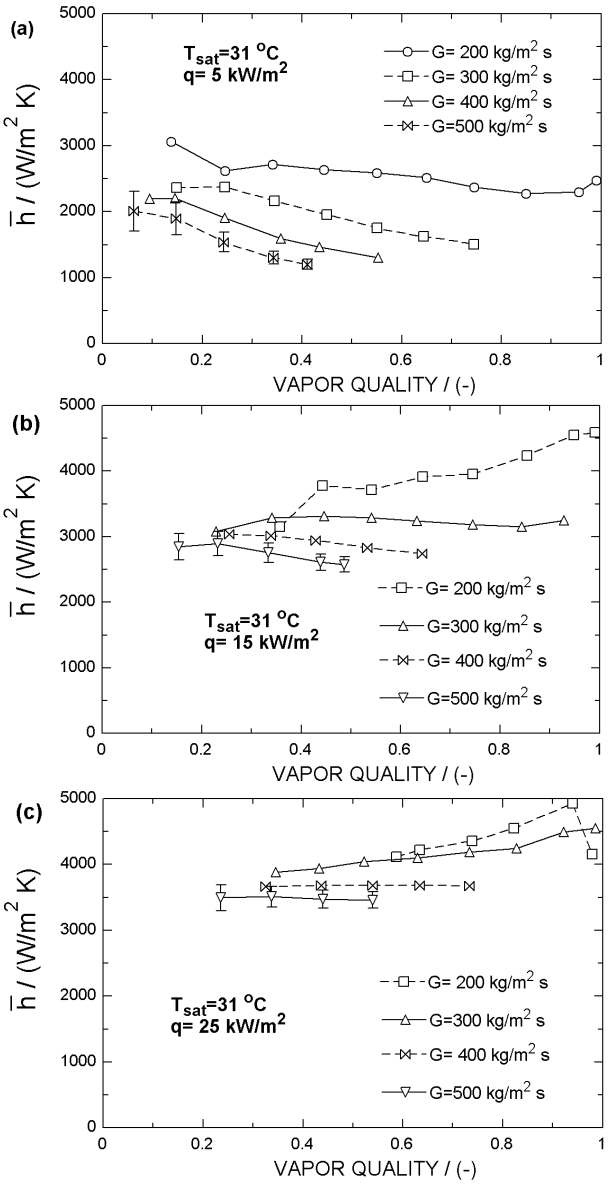

Figure 6. Illustration of the effect of the mass velocity on the heat transfer coefficient .

Saturation temperature. Figure 7 displays the effects of the saturation temperature on the heat transfer coefficient for G=100 kg/m^{2}s, q=15 kW/m^2 and saturation temperatures of 22, 31 and 41^{o}C. It can be noted that in general the effect of T_{sat} on the heat transfer coefficient

is marginal within the range of saturation temperatures evaluated in the present study.

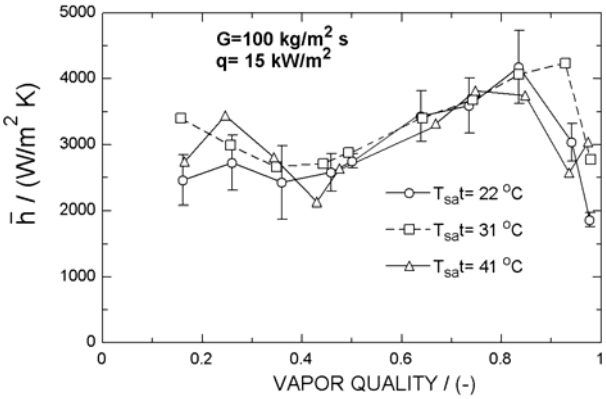

Figure 7. Illustration of the effect of the saturation temperature on the heat transfer coefficient.

Heat flux. According to Fig. 8, except for some of the results at vapor qualities higher than 0.9, the heat transfer coefficient increases with increasing the heat flux.

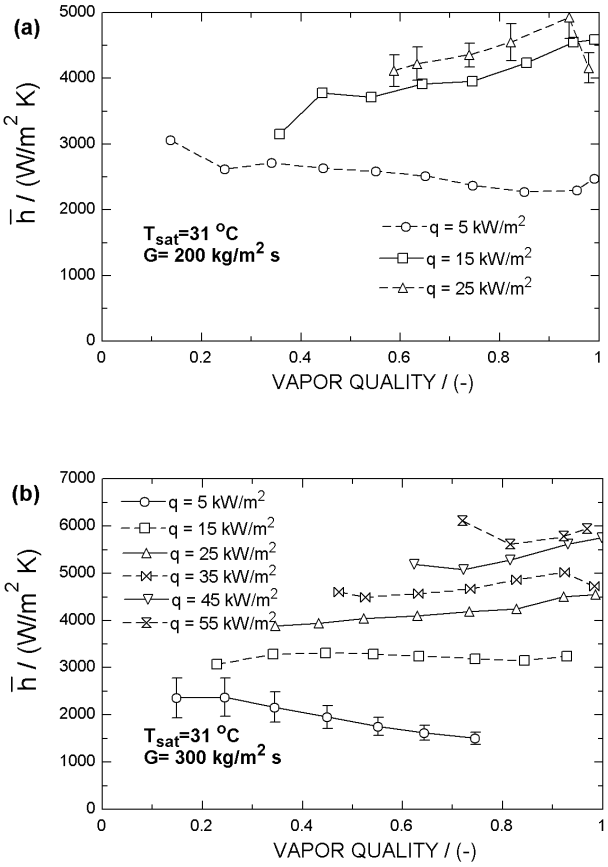

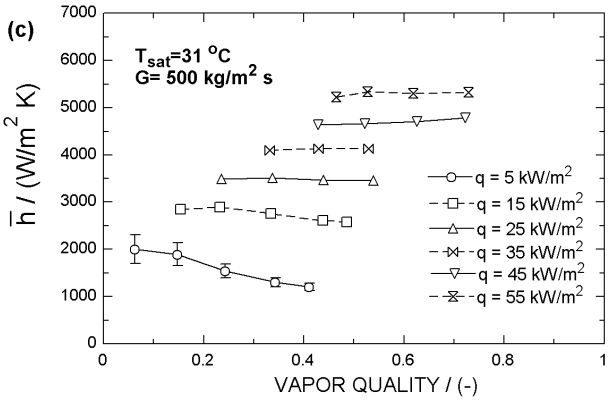

Figure 8. Illustration of the effect of the heat flux on the heat transfer coefficient.

Such a behavior differs from that observed in macro-scale channels according to which the heat transfer coefficient increases with increasing the heat flux but only at low vapor qualities and mass velocities. This behavior is related to the fact that nucleate boiling has been suggested as the dominant heat transfer mechanism in micro-scale channels. This statement comes from a misconception that an evaporation process dependent on the heat flux necessarily means that nucleate boiling is the controlling mechanism. Thome et al. (2004), for elongated bubble flow, and Qu and Mudawar (2003) for annular flow, have shown that the evaporation of a thin liquid film can also result in the heat transfer coefficient increasing with heat flux.

3.5 Comparison of the experimental data and predictive methods

In order to evaluate the capability of the current flow boiling prediction methods to predict the present database, a comparison between the experimental data and six flow boiling heat transfer prediction methods was performed. This comparison includes a total of 700 experimental data points with 175 of them having their flow pattern identified by high speed filming. The predictive methods are evaluated according to two criteria: the fraction of data predicted within ±30% error band, λ , and the mean absolute error, ε.

Table 2 depicts the statistics of the present comparison for the overall database. According to this table, Thome et al. (2004) method worked the best.

Figure 9 displays the distribution of the heat transfer coefficient vs. vapor quality in comparison to the heat transfer predictive methods for different experimental conditions. The heat transfer peak at low vapor qualities indicated by the 3-Zone model (Thome et al. (2004)) seems to occur according to the experimental results only in Fig. 9a, however, the heat transfer coefficient falloff at low vapor qualities with increasing vapor quality is much steeper than the one indicated by the 3-Zone model. Zhang et al. (2004) and Saitoh et al. (2007) predicted well the increase of the heat transfer coefficient with vapor quality at high vapor qualities displayed in Figs. 9a.

Table 2. Statistics of the comparison between the heat transfer predictions and the experimental data.

	PREDICTIVE METHOD					
	Zhang et al. (2004)	Thome et al. (2004)	Kandlikar and Balasubramanian (2004)	Liu and Winterton (1991)	Saitoh et al. (2007)	Bertscha et al. (2008)
ε (%)	51.2	**31.9**	46.9	33.4	39.8	37.2
λ (%)	49.4	**56.0**	31.6	51.8	43.6	48.9

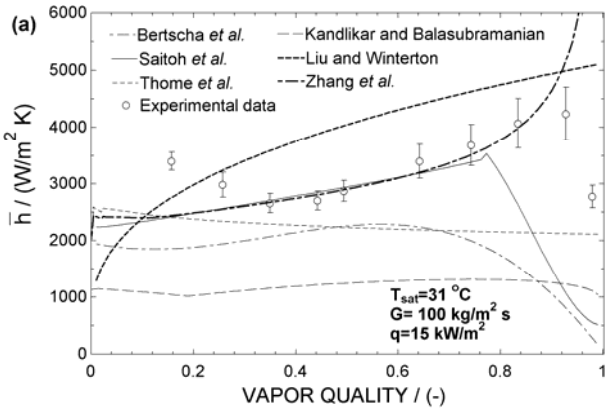

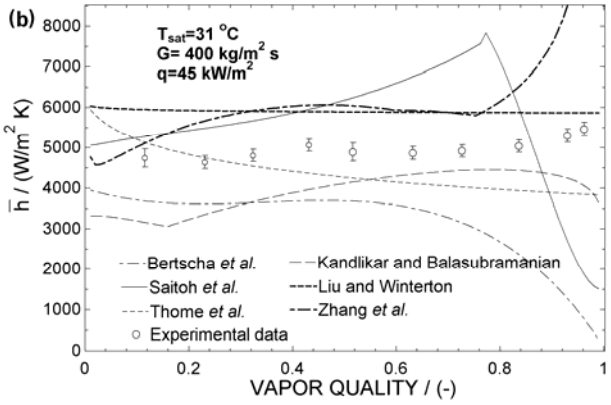

Figure 9. Heat transfer coefficient evolution with vapor quality according to the experimental data and predictive methods.

4. Conclusion

New accurate micro-scale flow boiling heat transfer data for R245fa in a 2.32mm circular tube were obtained and the main heat transfer behavior identified. The experimental data was parametrically analyzed and compared against predictive methods. The conclusion can be summarized as:

(1) Flow stratification was visualized and local wall temperature measurements revealed its effect on the circumferential variation of the heat transfer coefficient along the tube perimeter.

(2) Generally speaking, the heat transfer coefficient increases with heat flux. Distinct heat transfer behaviors with increasing vapor quality are observed according to the mass velocity. Saturation temperature presented a minor effect on the heat transfer coefficient. It was observed under certain experimental conditions that the heat transfer coefficient decreases with increasing the mass velocity.

(3) The predictive method proposed by Thome et al. (2004) worked the best and predicted the data with a average error of 32% but did not captured well most of the experimental heat transfer trends.

Acknowledgment

The authors gratefully acknowledge the financial support under contract numbers 05/60031-0, 06/52089-1 and 07/53950-5 given

by FAPESP (The State of São Paulo Research Foundation, Brazil). The technical support given to this investigation by Mr. José Roberto Bogni is appreciated and recognized.

Nomenclature

D	tube diameter, (m)
E	transferred energy to the tube (J)
G	mass velocity, (kg/m^{2}s)
h	heat transfer coefficient, (W/m^{2}K)
i	enthalpy (J/kg)
L	length, (m)
p	pressure, (Pa)
P	electrical power, (W)
q	heat flux (W/m^2)
Re	Reynolds number, (dimensionless)
T	temperature, (^{o}C)
x	vapor quality (-)
z	axial position (m)

Greek symbols

Δp	pressure drop
ε	mean absolute error (%)
λ	data points with in 30% error (%)

Subscripts

bottom	bottom of the tube
exit	exit of the test section
exp	experimental
inlet	inlet of the pre heater
local	at a specific position on the tube
middle	middle of the tube
sat	saturation temperature
top	top of the tube
w	inner wall temperature

References

Abernethy, R.B., Thompson, J.W., 1973, Handbook of uncertainty in gas turbine measurements, Arnold Engineering Development Center, Arnold Air Force Station, Tennessee.

Bertsch, S.S., Groll, E.A., Garimella, S.V., 2008, A composite heat transfer correlation for saturated flow boiling in small channels, Int. J. Heat Mass Transfer, 52, (7-8), 2110-2118.

Consolini, L., Ribatski, G., Wei, Z., Xu, J., Thome, J.R., 2007, Heat transfer in confined forced flow-boiling. Heat Transfer Eng. 28, 826-833.

Gnielinski, V., 1976, New equations for heat and mass transfer in turbulent pipe and channel from, Int. Chem. Eng. 16, 359-368.

Hetsroni, G., Mosyak, A., Pogrebnyak, E., Segal, Z., 2005, Explosive boiling of water in parallel micro-channels, Int. J. Multiphase Flow, 31, 371-392.

Kandlikar, S.G., Balasubramanian, P., 2004, An extension of the flow boiling correlation to transition, laminar, and deep laminar flows in minichannels and microchannels, Heat Transfer Eng. 25, 86–93.

Liu, Z., Winterton, R.H.S., 1991, A general correlation for saturated and subcooled flow boiling in tubes and annuli based on a nucleate pool boiling equation, Int. J. Heat Mass Transfer 34, 2759–2766.

Lowdermilk, W., Lanzo, C., Siegel, L., 1958, Investigation of boiling burnout and flow stability for water flowing in tubes, NACA. TN 4382.

Moffat, R.J., 1988, Describing the uncertainties in experimental results, Exp. Thermal Fluid Sci. 1, 3-17.

Qu, W., Mudawar, I., 2003, Flow boiling heat transfer in two-phase micro-channel heat sinks—II. Annular two phase flow model, Int. J. Heat Mass Transfer 46, 2773–2784.

Saitoh, S., Daiguji, H., Hihara, H., 2007, Correlation for boiling heat transfer of R-134a in horizontal tubes including effect of tube diameter, Int. J. Heat Mass Transfer 50, 5215–5225.

Thome, J.R., Dupont, V., Jacobi, A.M., 2004, Heat transfer model for evaporation in microchannels, part I: presentation of the model, Int. J. Heat Mass Transfer 47, 3375–3385.

Tibiriçá, C. B., Ribatski, G. 2009. An experimental study on micro-scale flow boiling heat transfer In: Boiling 2009. Florianópolis, SC, Brazil, 3-7 May.

Zhang, W., Hibiki, T., Mishima, K., 2004, Correlation for flow boiling heat transfer in mini-channels, Int. J. Heat Mass Transfer 47, 5749– 5763.